

Robust Positioning and Navigation of a Mobile Robot in an Urban Environment Using a Motion Estimator

Jongwoo An, and Jangmyung Lee*

Department of Electrical and Electronic Engineering, Pusan National University, Busan 46241, South Korea. E-mail: jongwoo7379@pusan.ac.kr

(Accepted December 22, 2018. First published online: February 20, 2019)

SUMMARY

Robust positioning and navigation of a mobile robot in an urban environment is implemented by fusing the Global Positioning System (GPS) and Inertial Navigation System (INS) data with the aid of a motion estimator. To select and isolate malicious satellite signals and guarantee the minimum number of GPS signals for the localization, an enhanced fault detection and isolation (FDI) algorithm with a short-term memory has been developed in this research. When there are sufficient satellite signals for positioning, the horizontal dilution of precision (HDOP) has been applied for selecting the best four satellite signals to localize the mobile robot. Then, the GPS data are fused with INS data by a Kalman filter (KF) for a straight path and a curved motion estimator (CME) for a curved path. That is, the INS data are properly fused to the GPS data through the KF or CME process. To verify the effectiveness of the proposed algorithm, experiments using a mobile robot have been carried out on a university campus.

KEYWORDS: GPS; INS; HDOP; Enhanced FDI; Motion estimator.

1. Introduction

Outdoor positioning is a core technology for airplanes, ships, and automated ground vehicles, and it will have a wider range of application areas in the future with the Internet of Things. Accurate information regarding outdoor locations can be easily obtained using the Global Positioning System (GPS).^{1–3} There are 28 GPS satellites in orbit over 20,200 km over the earth, each continuously transmitting an intrinsic signal with a time tag. Using the attitude and latitude information of the satellite and satellite time, GPS positioning becomes possible. That is, using four GPS satellite signals among the 24 satellites in the orbit, the location of a receiver on the earth can be computed by a trilateration method using the travelling time of the signals, which can be converted to the distance from a satellite to the object.^{4,5}

There are many applications for GPS positioning because the GPS orbit covers the whole world at any time.^{6,7} However, several error sources exist in GPS signal transmission, such as satellite orbit, satellite time, ionic layer delay, convective zone delay, multipath, and the GPS receiver. Because of error sources, it is not easy to compute the precise position of a receiver.^{8,9} Therefore, analysing received GPS signals to compensate for errors and exclude contaminated ones is necessary for localizing any type of mobile platform.¹⁰

In this research, the fault detection and isolation (FDI) scheme has been enhanced to incorporate the special environment in which satellite signals are neither highly reliable nor highly available. The FDI is a scheme to delete bad sensor data from the received GPS signal, which are caused by the weather conditions or interferences on the transmission path.¹¹ By deleting the bad data, the

* Corresponding author. E-mail: jmlee@pusan.ac.kr

reliability of the GPS positioning system can be improved. However, the compensation for the bad data itself has not been considered in the positioning. To overcome this problem, a multiple sensor fusion algorithm has been proposed in the recent researches.^{12,13}

It should be noted that the conventional FDI scheme depends strongly on the signal-to-noise ratio (SNR). To improve positioning accuracy in a hostile environment, such as in a dense of buildings, the measurement quality indicator (mesQI) and Doppler shift need to be checked in excluding the received GPS signal.^{14–16} When there are enough satellite signals after the enhanced FDI process, the horizontal dilution of precision (HDOP) can be utilized to select the best set of satellite signals for positioning.^{17,18}

In many cases, relying on GPS satellite signals alone is not good enough for successful localization and navigation. In such situations, the Inertial Navigation System (INS) has been utilized with GPS signals.¹⁹ The INS is very precise for a short time, and it can be utilized for the navigation of a mobile robot. However, it is basically a dead reckoning sensor system, which suffers drift or offset for long-term applications.²⁰

The INS is very effective for the localization of a mobile vehicle in GPS shadow areas where GPS signals are very weak and difficult to utilize. However, the INS data aggregate the dead reckoning errors, which becomes very serious in curved regions where the slippage of the wheels causes high-sensing errors. There have been several studies on error elimination in curved regions, and solutions have been suggested, such as position estimation using curvature motion.^{21–23} Curvature motion is defined as a centre of rotation (CR) and a rotation radius, which defines the motion trajectory of a mobile robot. In this paper, a method for precise motion control of a mobile robot is proposed using the enhanced FDI scheme and curved motion estimator (CME).

This paper comprises five sections, including this introduction. GPS navigation and positioning systems for positioning a mobile platform are introduced in Section 2. A new robust positioning algorithm is proposed with the enhanced FDI algorithm and the motion estimator in Section 3. In Section 4, the experiment conducted to verify the effectiveness of the proposed robust positioning and navigation algorithm is presented, and the data are analysed. Finally, conclusions and future works are discussed in Section 5.

2. GPS Positioning and Navigation Requirements

2.1. Point positioning with code range

The GPS receiver collects a few satellite signals to estimate the attitude, latitude, and height of the receiver itself using the relative distances to the GPS satellites. This measurement scheme is a point positioning which is relatively cheap and has a coarse accuracy. To improve the point positioning accuracy, pseudo code, carrier phase, and Doppler data can be utilized. At time t , the pseudo distance can be defined as

$$R_i^j(t) = \rho_i^j(t) + c\Delta\delta_i^j(t) \quad (1)$$

where $R_i^j(t)$ represents the measured pseudo-distance between measuring point i and satellite j , $\rho_i^j(t)$ is the geometrical distance between receiver i and satellite j , and c is the speed of light. Here, $\Delta\delta_i^j(t)$ is the time difference between the GPS reference and the receiver clocks.

In the geometrical distance $\rho_i^j(t)$, the position of the receiver at time t in the Earth-centred Earth-fixed (ECEF) coordinates, $X_i(t)$, $Y_i(t)$, and $Z_i(t)$ can be derived as

$$\rho_i^j(t) = \sqrt{(X^j(t) - X_i)^2 + (Y^j(t) - Y_i)^2 + (Z^j(t) - Z_i)^2} \quad (2)$$

where $X^j(t)$, $Y^j(t)$, and $Z^j(t)$ represent the known position of the j th satellite in ECEF coordinates.

The GPS satellite signal has a modulated carrier wave, which includes the followings:

1. A pseudorandom digital code that is known to the receiver. By time aligning between a receiver-generated and the receiver-measured versions of the code, the time of arrival (TOA) can be found in the receiver clock time scale.
2. A message that includes the time of code transmission (TOT) in GPS time scale and the satellite position at that time.

Conceptually, the receiver can estimate the travel time of the signal by the difference between the TOA in its own clock and the TOT in the GPS time scale. Since the receiver location can be specified by its three-dimensional position, three satellite signals are necessary for localization of the receiver. However, an additional satellite signal is required to compensate for the clock deviation between the receiver and the satellite.

In practice, the receiver position in the three-dimensional coordinates of latitude, longitude, and height in WGS83 (World Geodetic System) can be estimated simultaneously by using the obtained position in ECEF coordinates and the offset compensation between the receiver clock and the GPS time.^{24–26}

2.2. Navigation requirements

Navigation of a mobile robot starts from a well-known position and moves toward a desired position; great accuracy in approaching the desired position is normally required. To reach the goal position precisely and to avoid any undesirable collision with objects, the travelling path must be carefully planned and controlled through precise positioning during navigation. Several factors cause errors in GPS positioning and navigation systems, including satellite orbit error, satellite time error, ionospheric group delay, tropospheric group delay, multipath, receiver errors, selective availability, and the geometrical formation of satellites.^{27,28} To improve the positioning accuracy of the GPS receiver, these noise sources need to be cancelled out. For the cancellation or compensation of satellite signals, rigorous analysis of the satellite signal is required.

There are four major navigation requirements to assess the performance of satellite navigation systems: accuracy, integrity, continuity, and availability. These factors are critical to the performance of satellite navigation systems, because these factors are very closely related to positioning accuracy improvement, stability, and reliability as summarized below:

1. Accuracy is represented by the distance estimation error between the satellite and the GPS receiver, which is one of the most important, easy, and widely used requirements. To evaluate the accuracy, the receiver can be located at a precisely known location to estimate the location using the GPS signals. The weight of this accuracy is approximately 95% for the positioning system; it is directly related to the other three performance requirements.
2. Integrity is the function that alerts the user when the navigation system cannot achieve the required performance for a certain period of time. The loss of integrity occurs when the system does not notify a user regarding its own malfunction even though it found its faults. A system malfunction alarm includes the current malfunctioning of the system itself and the possible failure of the system in the near future, such as a large positioning error.
3. Continuity is an index that represents whether the role of the positioning system can be maintained continuously. When there is a loss of continuity in the positioning system, the final positioning cannot be completed even though the initial positioning is started successfully. This occurs when an integrity error is detected in the system and when the receiver does not operate properly and stops.
4. Availability indicates whether the role of the positioning system can be performed while the requirements are satisfied. Loss of availability can occur when the operation of the navigation system is stopped, localization is not possible because of a lack of feasible satellite signals, and the system failure is detected by the integrity test. The failure cannot be separated and recovered.

To improve not only the accuracy but also the other three performance indices, the enhanced FDI algorithm has been further improved with s short-term stack.

3. Enhanced FDI Algorithm

The minimum number of satellite signals is a critical factor for successful localization of the receiver. The conventional FDI algorithm²⁹ strongly depends on the SNR value, which may not guarantee the minimum number of satellite signals in a hostile environment. To improve the positioning accuracy, a reference station has been utilized to provide differential corrections and integrity monitoring for the receiver in the differential GPS (DGPS) and ground-based augmentation system (GBAS). However, in many industrial applications, DGPS or GBAS is too expensive to apply to the localization of a mobile robot.

In this research, a short-term stack has been added to the enhanced FDI algorithm to improve the localization accuracy using a commercial GPS receiver. The short-term stack, S^i , has been

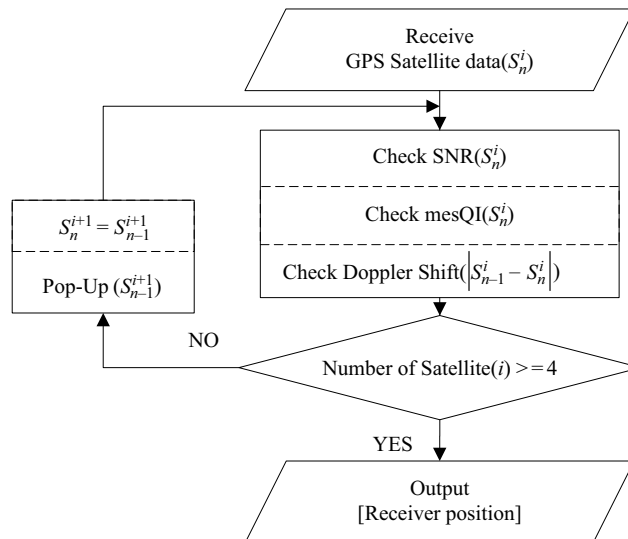


Fig. 1. The enhanced FDI algorithm with a short-term stack.

implemented for the i th satellite signal to keep the satellite signal in a time sequence, which is used to pop up a new satellite signal when the current satellite signal is not suitable for the localization. The stack size, n , needs to be determined heuristically considering the speed of the mobile robot (equally the receiver) and the accuracy requirement for the system.

As shown in Fig. 1, when the SNR is greater than 20 dB, the satellite signal is passed to the next step. In the second step, the mesQI value of each satellite signal is checked. The satellite signal is compared to the previous data to confirm the mesQI, which is a data-quality-monitoring index. The normal mesQI value is greater than four for a U-Blox GPS receiver. Therefore, when a satellite signal has a mesQI value smaller than four, it is excluded from the localization. Finally, the Doppler shift of each signal is checked, which represents the relative velocity between the satellite and the receiver. When the receiver is stationary, the Doppler shift should be constant because the satellite is on the stationary earth orbit. If it is not constant, the received satellite signal might be an indirect one, which must be excluded from the localization. This Doppler shift is a good index to represent the quality of the received satellite signal when the receiver is stationary or moving very slowly.

In addition to these three steps, a short-term stack is applied for the localization. Even after these three steps of the rigorous detection and isolation process, there could be a strong possibility of not having enough satellite signals for localization. When this occurs, a short-term stack for the excluded satellite signal, S_n^i , which is i th satellite signal at the n th time instance, is activated to pop up the signal S_{n-1}^i to replace the malicious S_n^i . This idea is very effective for stationary and slowly moving receivers. Note that the stack size should be selected to be small enough not to cause inaccurate localization. Therefore, even though this short-term stack is very effective to keep more reliable satellite signals, it cannot guarantee enough satellite signals at all times.

The localization accuracy improvement by the enhanced FDI with a short-term stack has been shown by the comparison of circular error probability (CEP) and twice-distance root-mean-square (2DRMS) values with the conventional FDI in Figs. 2 and 3. This experiment has been performed for 15 min by receiving GPS data every 1 s near at a building to simulate the urban environment. Focusing on the obstacles in the transmission path of the GPS signals, the experiments are performed during the sunny daytime without considering weather conditions.

The CEP represents the radius of a circle which includes 50% data inside the circle. The CEPs for the conventional FDI and the enhanced FDI with a short-term stack are 19.74 and 16.23 m, respectively. The 2DRMS represents the radius of a circle which includes 95% data inside the circle, whose values for the conventional FDI and the enhanced FDI with a short-term stack are 45.00 and 38.91 m, respectively.

4. Proposed Algorithm for Robust Positioning

The navigation of a mobile robot in an urban area can be modelled as a straight path or a curved path. Generally, Kalman filter (KF) is used to improve the accuracy of GPS data in localization, which is

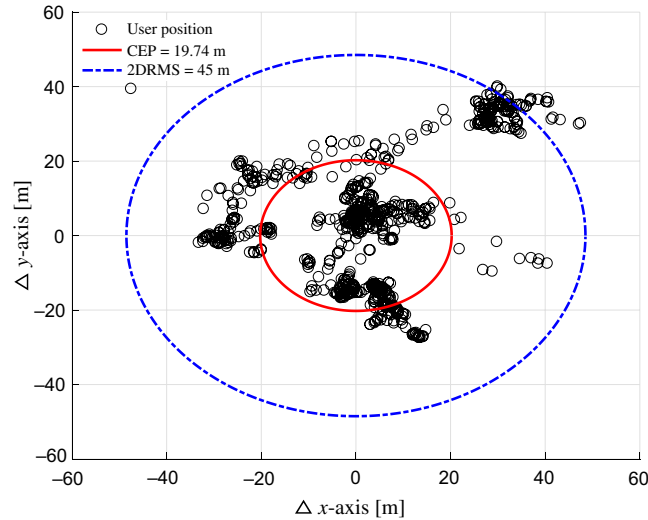


Fig. 2. Localization error by conventional FDI.

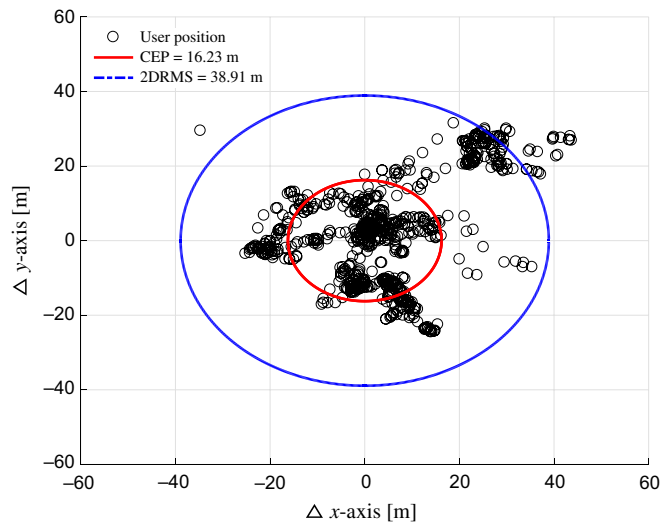


Fig. 3. Localization error by enhanced FDI with a short-term stack.

especially effective for a straight path. For a curved path, which can be represented by CR and the rotation radius, in this research, CME has been developed and implemented to improve the accuracy of the GPS data for localization.

4.1. Straight path estimation using KF

The GPS data in the straight line region can be improved by fusion with INS data through the KF. The multivariable discrete system can be represented as discrete state equations as follows:

$$\begin{aligned} x_{k+1} &= Ax_k + w_k \\ z_k &= Hx_k + v_k \end{aligned} \quad (3)$$

where x_k is a 9×1 state vector formed by the state variables to represent the position, velocity, and RPY (Roll, Pitch, Yaw) angles of the receiver. Here, z_k is a 9×1 observation vector, which is composed of the position (latitude, longitude, altitude) and velocity of the mobile robot measured by the GPS signals, and the roll, pitch, and yaw angles measured by the IMU sensor. The matrix A is a 9×9 state transition matrix, H is a 9×9 observation matrix, and w_k and v_k represent process and measurement noise vector, respectively.

Along a straight path, the GPS data for mobile robot localization can be estimated and adjusted by the KF process illustrated in Fig. 4. In the first step, state variables \hat{x}_0 and error covariance matrix U_0

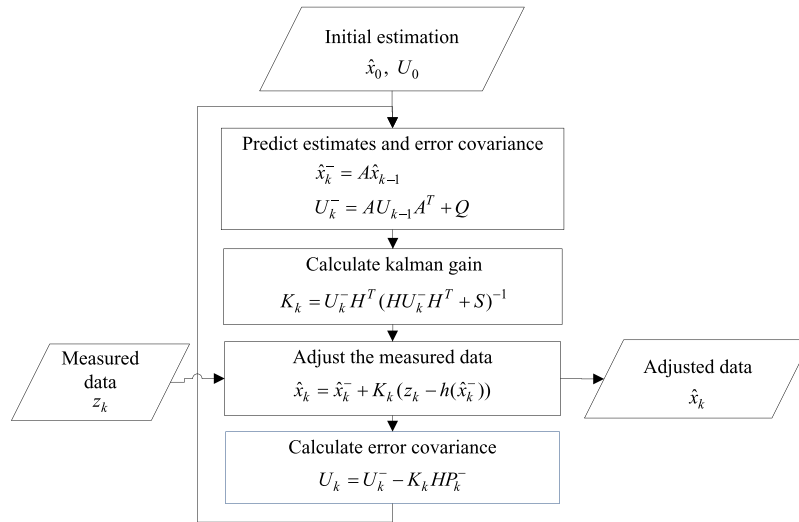


Fig. 4. KF procedure for the estimation of the mobile robot position.

are initialized. In the second step, the state vector \hat{x}_k and error covariance matrix U_k are estimated. Here, Q represents the error covariance matrix of system noises w_k , which is defined as

$$Q = \text{diag}(\sigma_{f_x}^2, \sigma_{f_y}^2, \sigma_{f_z}^2, 0, 0, -9.8, \sigma_{\omega_x}^2, \sigma_{\omega_y}^2, \sigma_{\omega_z}^2) \tag{4}$$

where $(\sigma_{f_x}^2, \sigma_{f_y}^2, \sigma_{f_z}^2)$ represents the variance of the accelerations measured by the IMU sensor, $(0, 0, -9.8)$ represents the gravity component, and $(\sigma_{\omega_x}^2, \sigma_{\omega_y}^2, \sigma_{\omega_z}^2)$ represents the variance of angular velocities also measured by the IMU sensor.

In the third step, the Kalman gain is computed. The matrix S represents the error covariance matrix of the measurement noises v_k , which is defined as follows:

$$S = \text{diag}(\sigma_{r_x}^2, \sigma_{r_y}^2, \sigma_{r_z}^2, \sigma_{v_{gps}}^2, 0, 0, \sigma_{\phi}^2, \sigma_{\theta}^2, \sigma_{\psi}^2) \tag{5}$$

where $(\sigma_{r_x}^2, \sigma_{r_y}^2, \sigma_{r_z}^2)$ and $(\sigma_{v_{gps}}^2, 0, 0)$ represent the variance of the mobile robot position and velocity measured by GPS signals, respectively. Here, $(\sigma_{\phi}^2, \sigma_{\theta}^2, \sigma_{\psi}^2)$ represents the variance of Euler angles of the mobile robot measured by the IMU sensor.

In the fourth step, the measured data are adjusted by using the Kalman gain K_k and the transformation function $h(\hat{x}_k^-)$. That is, the malicious GPS data are adjusted with the fusion of INS data. In the last step, the error covariance matrix U_k is updated for the next loop operation.

4.2. CME algorithm

Figure 5 presents a possible path for the mobile robot to move along toward a desired position and orientation. A straight path, which has an infinite rotation radius R , is the best for the mobile robot for precise tracking without slippage. However, in many cases, curved motion is required as shown in Fig. 5. Therefore, in the trajectory planning, a curved path that has the bigger rotation radius is desirable if it can be achieved. The rotation radius R , based on its instantaneous centre of rotation (ICR), can be defined as

$$R = \frac{L}{2} \left(\frac{v_R + v_L}{v_R - v_L} \right) \tag{6}$$

When the mobile robot moves from point P_0 (time = t) to point P_1 (time = $t + \Delta t$), and its locations are given as (x_p, y_p, θ) and (x'_p, y'_p, θ') , respectively, the coordinates of the ICR can be expressed as

$$\text{ICR} = [x_p - R \cdot \sin \theta, y_p + R \cdot \cos \theta] \tag{7}$$

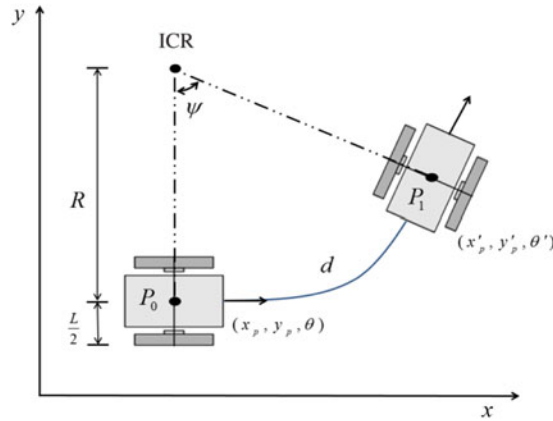


Fig. 5. Curved motion of a mobile robot.

For a given time difference of Δt from t , the location of the mobile robot (x'_p, y'_p, θ') is expressed by using the location and angular velocity of the mobile robot as well as the location of its ICR as

$$\begin{aligned} \begin{bmatrix} x'_p \\ y'_p \\ \theta' \end{bmatrix} &= \begin{bmatrix} \cos(\psi \cdot \Delta t) & -\sin(\psi \cdot \Delta t) & 0 \\ \sin(\psi \cdot \Delta t) & \cos(\psi \cdot \Delta t) & 0 \\ 0 & 0 & 1 \end{bmatrix} \begin{bmatrix} x_p - ICR_x \\ y_p - ICR_y \\ \theta \end{bmatrix} + \begin{bmatrix} ICR_x \\ ICR_y \\ \psi \cdot \Delta t \end{bmatrix} \\ &= \begin{bmatrix} R \sin(\psi \cdot \Delta t) + ICR_x \\ -R \cos(\psi \cdot \Delta t) + ICR_y \\ \theta + \psi \cdot \Delta t \end{bmatrix} \end{aligned} \tag{8}$$

Furthermore, the numerical expressions of the total moving distance d of the mobile robot from P_0 to P_1 and the change of heading angle ψ are expressed as

$$d = \int_t^{t+\Delta t} \frac{v_L + v_R}{2} dt \tag{9}$$

$$\psi \left(= \frac{d}{R} \right) = \frac{\int_t^{t+\Delta t} (v_L + v_R) dt}{L(v_L + v_R)} (v_R - v_L) \tag{10}$$

The above equations can be used to measure the radius of the rotation, the moving distance, the rotational angle, as well as the linear and rotational velocities of the mobile robot. During the curvature motion y , the GPS data are adjusted to fit onto the curvature path represented by R and ICR.

A single curvature trajectory is not always possible depending on the direction of the mobile robot and the moving object. Referring to Fig. 6 and Eqs. (9) and (10), the condition for a single curvature can be defined as follows. When the change of heading angle $\psi (= \theta' - \theta)$ is negative, P_1 should be located on the right side of the extended path along the θ direction (shadow area in Fig. 6). If ψ is positive, P_1 should be located on the left side of the path. When this condition is not satisfied, a double curvature trajectory needs to be planned, which has two curvatures with smaller rotation radii than the single curvature path.

It should be noted that generating a path that has a maximum rotation radius is a critical factor in achieving precise control of a mobile robot. Moreover, when ψ is zero, the rotation radius becomes infinite unless the travelling distance d is zero. Therefore, when ψ is zero, a double curvature path is required to reach the goal.

4.3. Robust positioning using motion estimation

Figure 7 illustrates the robust localization algorithm proposed in this paper. After the enhanced FDI, which guarantees the minimum number of satellite signals to be used for localization, the HDOP process is applied to select the best combination of GPS data sets. When there is no set that satisfies the threshold value (it was selected as 3 in this research) of the HDOP, the process goes back to the

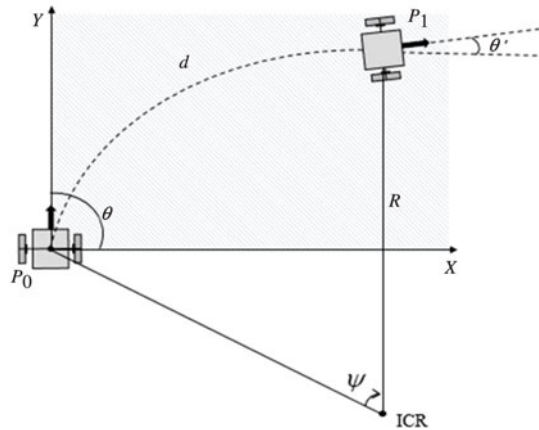


Fig. 6. Condition for a single curved path.

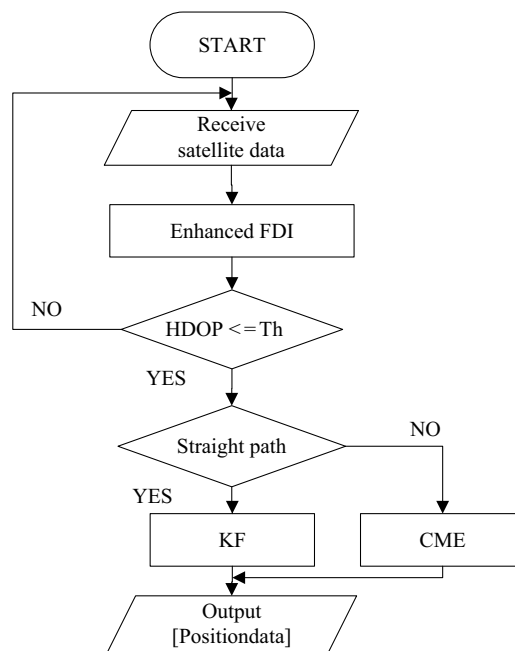


Fig. 7. Flowchart for the proposed robust positioning and navigation algorithm.

data-gathering step. The final GPS data sets are adjusted by the KF for a straight path and by the CME for a curved path. The classification of a path as either straight or curved is based upon the encode data at the wheels of the mobile robot. That is, when the encode values of the left and right are the same, the path is assumed to be straight. When there is a discrepancy between the two sets of data, the CR and the rotation radius are estimated to be used in the CME process. By the modification of the malicious GPS signal to be good, the localization accuracy of the mobile robot can be improved.

5. Navigation Experiments and Discussions

5.1. Construction of hardware and experiments

To construct a positioning system for a mobile platform, a GPS receiver, IMU sensor, and notebook PC are installed on a mobile platform as shown in Fig. 8. The GPS receiver used for this experiment was the EVK-6T from u-Blox Corporation. The IMU sensor model is EBIMU-9DOFV3 made by E2BOX Corp. Using this experimental system, the efficiency of the proposed robust positioning algorithm was verified. A KF was utilized to improve the accuracy in the straight line region with the experimentally obtained error covariance matrix of system noises and the error covariance matrix of measurement noise.

Table I. System and measurement noises for KF.

Item	Value
System noise	$Q = \text{diag}(0.007 \ 0.004 \ 0.004 \ 0 \ 0 \ -9.81 \ 0.1 \ 0.112 \ 0.796)$
Measurement noise	$S = \text{diag}(2.851 \ 2.359 \ 1.721 \ 0.002 \ 0 \ 0 \ 7 * 10^{-4} \ 0.002 \ 0)$

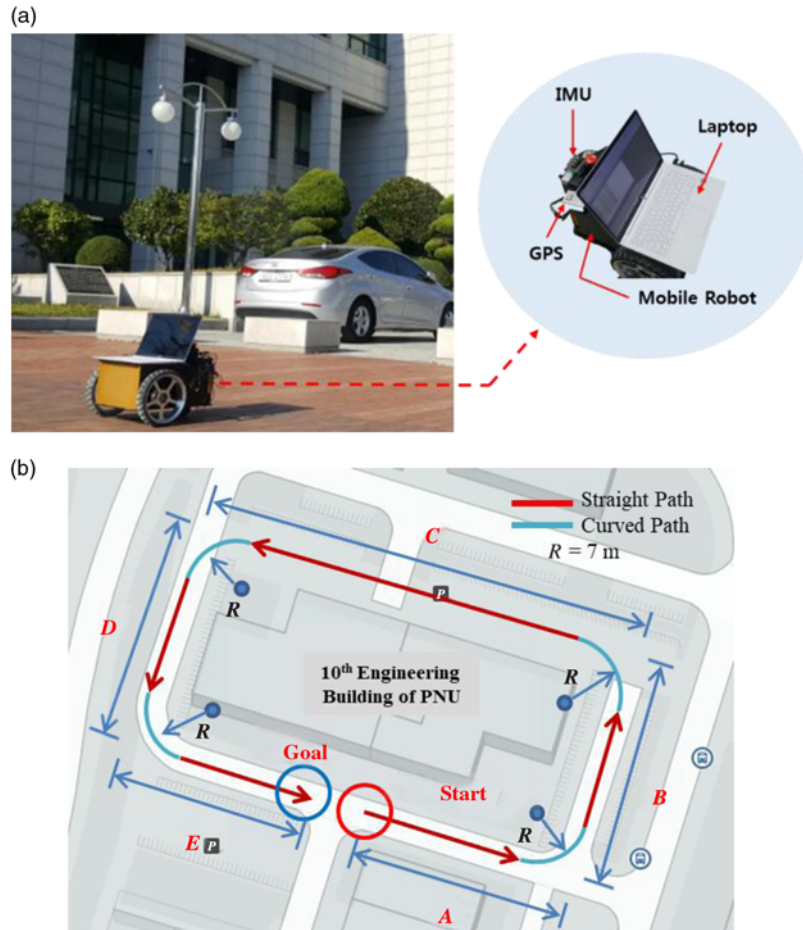


Fig. 8. Experimental environment for mobile robot navigation. (a) Experimental mobile robot. (b) Combination of straight and curved paths.

System and measurement noises are specified in Table I.

For the curved region, as shown in Fig. 8(b), the CME algorithm was applied to keep the same rotation radius w.r.t the CR to improve the position estimation accuracy.

An entrance of a building was selected for the location of the mobile robot, where the GPS signals could be blocked and distorted by the walls. In this hostile environment, the performance of the proposed robust positioning algorithm was verified and assessed in comparison to enhanced FDI.

5.2. Navigation results on the campus

Figure 9 shows the experimental results of navigation in the urban environment as shown in Fig. 8. The reference path is represented by the dashed red line. The black, green, and blue lines represent the experimental navigation paths by conventional FDI, enhanced FDI, and the proposed algorithm, respectively.

It is noted that the localization error in the region C in Figs. 9 and 10 is very large by the conventional FDI algorithm. Actually there is a neighbouring building in the region C, which causes the interferences in the GPS signals. As the minimum contribution of this paper, the localization error has been reduced to the same level of other regions by the proposed algorithm as shown in Fig. 10.

As seen in Fig. 10, the enhanced FDI algorithm²⁰ also improves the navigation accuracy in comparison to the conventional FDI algorithm.²⁹ In the proposed algorithm, a short-term stack has

Table II. Comparison of localization errors.

Item	Minimum Position Error [m]	Maximum Position Error [m]
Conventional FDI	0.92	39.61
Enhanced FDI	0.82	12.58
Proposed Algorithm	0.61	4.91

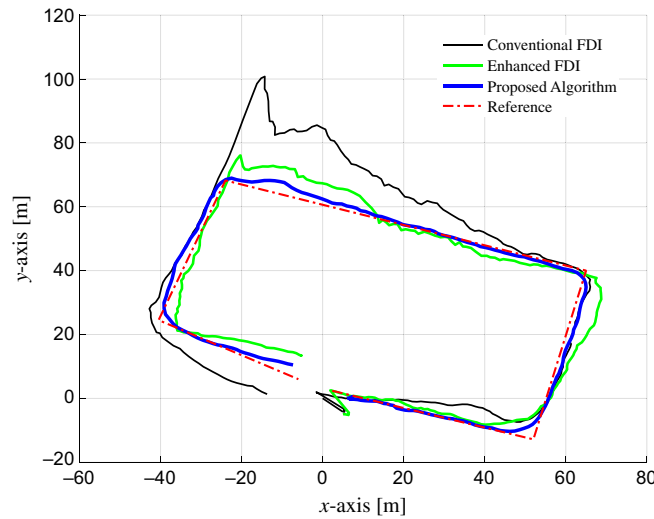


Fig. 9. Experimental navigation.

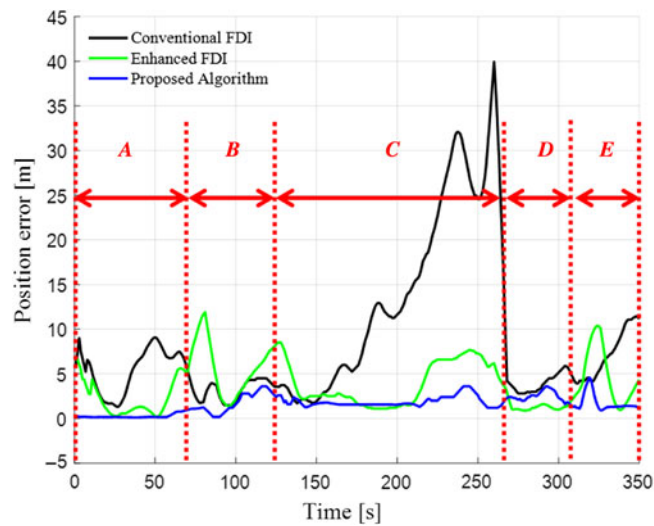


Fig. 10. Comparison of localization/navigation errors.

been added to the enhanced FDI and the malicious GPS data have been fused with INS data by the KF or CME. It can be concluded that this proposed algorithm can keep the navigation error smaller than 5 m in most of urban environments. The navigation errors for each algorithm in Fig. 10 are analysed and summarized in Table II.

6. Conclusions

A new robust positioning scheme has been implemented by fusing GPS and INS data signals with a motion estimator in hostile environments, and its effectiveness has been verified in this research. GPS signals are distorted and contaminated by interferences when the mobile robot is navigated near

a building, which makes the accuracy of localization of a mobile robot very poor. To overcome this problem, the robust positioning algorithm uses a motion estimator which applies the KF for a straight path and the CME for a curved path. For the robust positioning method, the enhanced FDI algorithm has been also adopted with the HDOP. Through experiments, it was verified that the robust positioning algorithm proposed in this research can be utilized to localize a mobile robot using GPS and INS data in a hostile environment. In future research, the algorithm may need to be improved with the utilization of INS to incorporate high-speed mobile platforms, such as automobiles.

Acknowledgments

This research was funded and conducted under the Competency Development Program for Industry Specialists of the Korean Ministry of Trade, Industry and Energy (MOTIE), operated by Korea Institute for Advancement of Technology (KIAT) (No. N0001126, HDR program for Industrial convergence/connected for creative robot human resource development).

This research was a part of the project titled ‘Developments of Drone Docking System equipped Leisure Boat for Drone surfing and operating’, funded by Ministry of Oceans and Fisheries, Korea.

References

1. S. J. Lee, G. Tewolde and J. R. Kwon, “Design and Implementation of Vehicle Tracking System Using GPS/GSM/GPRS Technology and Smartphone Application,” *Proceedings of IEEE World Forum on Internet of Things (WF-IoT)*, Seoul, Korea (2014) pp. 353–358.
2. J. Foster, N. Li and K. F. Cheung, “Sea state determination from ship-based geodetic GPS,” *J. Atmos. Oceanic Technol.* 31(11), 2556–2564 (2014).
3. P. Pramod, “GPS based advance soldier tracking with emergency messages and communication system,” *Int. J. Adv. Res. Comput. Sci. Manag. Stud. Res. Art.* 2(6), 25–32 (2014).
4. X. Li, G. Dick, M. Ge, S. Heise and J. Wickert, “Real time GPS sensing of atmospheric water vapor: Precise point positioning with orbit, clock, and phase delay corrections,” *Geophys. Res. Lett.* 40(10), 3615–3621 (2014).
5. V. Milanés, J. E. Naranjo, C. González, J. Alonso and T. de Pedro, “Autonomous vehicle based in cooperative GPS and inertial systems,” *Robotica* 26(5), 627–633 (2008).
6. S. R. Webb, N. T. Penna and P. J. Clarke, “Kinematic GNSS estimation of zenith wet delay over a range of altitudes,” *J. Atmos. Oceanic Technol.* 33(1), 3–15 (2016).
7. Q. Zhu, Z. Zhao and L. Lin, “Real time estimation of slant path tropospheric delay at very low elevation based on singular ground-based global positioning system station,” *IET Radar Sonar Navig.* 7(7), 808–814 (2013).
8. F. Chan, M. Joerger and B. Pervan, “Stochastic modeling of atomic receiver clock for high integrity GPS navigation,” *IEEE Trans. Aerosp. Electron. Syst.* 50(3), 1749–1764 (2014).
9. V. Pereira, A. Giremus and E. Grivel, “Modeling of multipath environment using copulas for particle filtering based GPS navigation,” *IEEE Signal Process. Lett.* 19(6), 360–363 (2012).
10. M. R. Azarbad and M. R. Mosavi, “A new method to mitigate multipath error in single-frequency GPS receiver with wavelet transform,” *GPS Solutions* 18(2), 189–198 (2014).
11. H. J. Kim, J. W. Song, C. W. Kang and C. H. Park, “FDI performance analysis of inertial sensors on multiple conic configuration,” *J. Korean Soc. Aeronaut. Space Sci.* 43(11), 643–951 (2015).
12. T. P. Banerjee and S. Das, “Multi-sensor data fusion using support vector machine for motor fault detection,” *Inf. Sci.* 217, 96–107 (2012).
13. A. Abid and M. T. Khan, “Multi-sensor, Multi-level Data Fusion and Behavioral Analysis Based Fault Detection and Isolation in Mobile Robots,” *Proceedings of 8th IEEE Information Technology, Electronics and Mobile Communication Conference*, Vancouver, BC, Canada (2017) pp. 40–45.
14. D. Qiao, Q. Cheng and Y. Hou, “Fault Detection and Isolation of Sensor in Time-delay Systems Based on Space Geometry Method,” *Proceedings of IEEE 11th Conference on Industrial Electronics and Applications (ICIEA)*, Hefei, China (2016) pp. 444–449.
15. W. Huang and X. Su, “Design of a fault detection and isolation system for intelligent vehicle navigation system,” *Int. J. Navig. Obs.* 2015 (2015).
16. V. Dehghanian, J. Nielsen and G. Lachapelle, “GNSS spoofing detection based on signal power measurements: Statistical analysis,” *Int. J. Navig. Obs.* 2012 (2012).
17. D. H. Won, J. Ahn, S. W. Lee and S. Sung, “Weighted DOP with consideration on elevation-dependent range errors of GNSS satellites,” *IEEE Trans. Instrum. Meas.* 61(12), 3241–3250 (2012).
18. M. Tahsin, S. Sultana and T. Reza, “Analysis of DOP and Its Preciseness in GNSS Position Estimation,” *Proceedings of IEEE International Conference on Electrical Engineering and Information Communication Technology (ICEEICT)*, Dhaka, Bangladesh (2015) pp. 1–6.
19. C. Onunka, G. Bright and R. Stopforth, “USV attitude estimation: An approach using quaternion in direction cosine matrix,” *Robotica* 34(5), 995–1009 (2016).
20. Y. K. Kim, J. W. An and J. M. Lee, “Robust navigational system for a transporter using GPS/INS fusion,” *IEEE Trans. Ind. Electron.* 65(4), 3346–3354 (2018).

21. S. Ghaffari and M. R. Homaeinezhad, "Autonomous path following by fuzzy adaptive curvature-based point selection algorithm for four-wheel-steering car-like mobile robot," *Proc. Inst. Mech. Eng. Part C: J. Mech. Eng. Sci.* 232(15), 2655–2665 (2018).
22. S. D. Murthy, S. Krishnan, G. Sundarajan, S. Kiran Kassyap, R. Bhagwanth and V. Balasubramanian "A Robust Approach for Improving the Accuracy of IMU Based Indoor Mobile Robot Localization," *Proceedings of 13th International Conference on Informatics in Control, Automation and Robotics*, Lisbon, Portugal, (2016) pp. 437–445.
23. T. S. Dao, K. Y. K. Leung, C. M. Clark and J. P. Huisson, "Markov-based lane positioning using intervehicle communication," *IEEE Trans. Intell. Trans. Syst.* 8(4), 641–650 (2007).
24. M. Kebaetse, P. McClure and N. A. Pratt, "Thoracic position effect on shoulder range of motion, strength, and three-dimensional scapular kinematics," *Arch. Phys. Med. Rehabil.* 80(8), 945–950 (1999).
25. P. Huang and Y. Pi, "An improved location service scheme in urban environments with the combination of GPS and mobile stations," *Wireless Commun. Mobile Comput.* 14(13), 1287–1301 (2014).
26. S. Duncan and T. I. Stewart, "Portable global positioning system receivers: Static validity and environmental conditions," *Am. J. Preventive Med.* 44(2), 19–29 (2013).
27. D. Sathyamorthy, S. Shafii and Z. F. M. Amin, "Valuating the Trade-off between Global Positioning System (GPS) Accuracy and Power Saving from Reduction of Number of GPS Receiver Channels," *Proceedings of IEEE International Conference on Space Science and Communication (IconSpace)*, Malaysia (2015) pp. 221–224.
28. M. S. Braasch, "Isolation of GPS multipath and receiver tracking errors," *Navigation* 41(4), 415–435 (1994).
29. E. Wang, C. Jia, G. Tong, P. Qu, X. Lan and T. Pang, "Fault detection and isolation in GPS receiver autonomous integrity monitoring based on chaos particle swarm optimization-particle filter algorithm," *Adv. Space Res.* 61(5), 1260–1272 (2018).